

Collaborative Resilience to Extreme Weather in Decentralized Co-operation of Electricity and Natural Gas Distribution Systems

Ahmad Nikoobakht^{1*}, Jamshid Aghaei², Mousa Afrasiabi², Vahid Vahidinasab³

¹Department of Electrical Engineering, Higher Education Center of Eghlid, Eghlid 0752422334, Iran (e-mail:

a.nikoobakht@eghlid.ac.ir)

²Department of Electrical Engineering, School of Energy Systems, Lappeenranta-Lahti University of Technology, FI-53850,

Lappeenranta, Finland (Jamshid.aghaei@lut.fi and mousa.afraziabi@lut.fi)

³Department of Engineering, School of Science and Technology, Nottingham Trent University, Nottingham NG11 8NS, UK

(email: vahid.vahidinasab@ntu.ac.uk)

*Corresponding Author: A. Nikoobakht (a.nikoobakht@eghlid.ac.ir)

Abstract— The flexibility of the power-to-gas (P2G) technologies and natural gas units (NGUs) can enhance the resilience of the electric distribution system (EDS) considering the high penetration of renewable energy resources (RERs). The decentralized collaborative operation (co-operation) of electric distribution systems and natural gas systems (EDS&NGSs) considering information privacy preserving can enhance the resilience during an extreme hurricane. To address this issue, this paper proposes a three-level hierarchal solution to decompose the centralized co-operation of the EDS&NGS framework in which an independent decision-making strategy and information privacy preserving for both network operators are simultaneously addressed. Furthermore, in this paper, a min–max robust resilience-constrained co-optimization model is presented to enhance the resilience of the integrated EDS&NGS against worst-case $N - k$ contingencies and wind power generation uncertainty under extreme hurricane events. To attain the spatial dynamics of extreme hurricanes, a the multi-zone and multi-time extreme hurricanes model is considered. Then, a column-and-constraints generation (C&CG) algorithm is used to solve the proposed robust resilience-constrained co-optimization model. To verify the effectiveness of the model, we conducted experiments on a modified IEEE-33-bus-10-node/123-bus-20-node EDS&NGS. The numerical results show that the proposed robust resilience-constrained co-operation of EDS&NGS problem is an effective model for enhancing EDS resilience.

Keywords— Resilience enhancement, distribution and natural gas networks, extreme renewable uncertainty, extreme hurricanes.

NOTATION

A. Indices

w	Index of wind turbine.
i, j	Index of electrical buses.
n	Index of gas node.
k	Index of distribution lines.
ν	Index of zone.
g	Index of NGU.
t	Index of hour.
χ_t / χ_r	Sets of response/target variable.
α^c / α^w	Uncertainty set of distribution line outage/load variations.
Π_0	Sets of total distribution lines.
Π_z	Set of distribution lines in the Zone Z .
Ψ_Z	Set of wind farms in the Zone Z .
$(\bullet)_{(\cdot),t}$	Related to element (\cdot) at time period t .

All variables and constants include the superscript Ω referring to before, $\Omega \in \{o\}$, and after, $\Omega \in \{r\}$, an extreme hurricane event.

B. Parameters

η_r	Number of distribution line outages in zone r .
Z	Number of total zones.
\bar{P}_{wt}	Wind power forecasted.
\hat{P}_{wt}	Variation range of wind power generation from wind power forecasted.
α_z	Robustness degree in zone z .
c_g	Generation cost of an NGU.
c_g^{su}	Start-up cost of an NGU.
$\underset{\cup}{c}_t$	Active power exchange cost at a substation.

UT / DT	Min time for on/off an NGU.
$\underline{P}_g / \bar{P}_g$	Min/max active power generation for an NGU.
\bar{Q}_g	Maximum reactive power generation for an NGU.
$\underline{\Delta r}_g / \bar{\Delta r}_g$	Min/max ramp-rate of an NGU.
g_k / b_k	Conductance/susceptance of a distribution line.
$\gamma_{ij} / \lambda_{ij}$	Slop/constant parameter.
$\bar{\varphi}$	Maximum phase angle limit across a distribution line.
$\underline{V}_i / \bar{V}_i$	Min/max voltage magnitude.
Q_{it} / P_{it}	Active/reactive load forecasted.
$1_{(g)}$	Dual variable resilience constraints.
U_n	Gas production cost for a gas well.
g_n	Cost of gas storage.
ζ_n	Gas unserved cost.
$\underline{G}_n / \bar{G}_n$	Min/max gas production for a gas well.
$\underline{\pi}_n / \bar{\pi}_n$	Min/max gas pressure at a node.
\bar{D}_{nt}	Residential (non-electrical) gas load.
η_{NGU}	Fuel coefficient of NGU.
Υ_{nm}, L_{nm}	Constants of a gas pipeline.
\mathcal{K}_{nm}	Line pack constant of a gas pipeline.
$\underline{S}_n^{in} / \bar{S}_n^{in}$	Min/max gas flow into a gas storage.
$\underline{S}_n^{ou} / \bar{S}_n^{ou}$	Min/max gas flow out of a gas storage.
η_{P2G}	Power to gas coefficient of P2G technology.
$\tau, \bar{\tau}$	Multipliers of penalty function.
\mathcal{E}	Acceptable error.

C. Variables

z_{kt}	Binary variable to specify outage for distribution line k at time t .
P_{wt}	Wind power generation.
Θ^{TC}	Total co-operation cost of EDS&NGS.
Θ^E / Θ^G	Total EDS/NGS operation cost.
P_t^Ω / Q_t^Ω	Active/reactive power exchange.
v_{gt} / w_{gt}	Start-up/shutdown binary variable for an NGU.
u_{gt}	Binary variable to show on/off for an NGU.
$P_{gt}^\Omega / Q_{gt}^\Omega$	Active/reactive power generation for a NGU.
$P_{ij,t}^\Omega / Q_{ij,t}^\Omega$	Active/reactive power flow on a distribution line.
V_{it}^Ω	Voltage magnitude at a bus.
$\phi_{ij,t}^\Omega$	Phase angle difference across a distribution line.
$\psi_{ij,t}^\Omega$	Auxiliary variable to define $\cos \phi_{ij,t}^\Omega$
$\theta_{ij,t}^\Omega / \theta_{ij,t}^\Omega$	Auxiliary variable to define active/reactive power flow on a distribution line.
P_{vt}^Ω	Active power consumed by P2G technology.
D_{nt}^Ω	Gas unserved.
$S_{nt}^\Omega / S_{nt}^\Omega$	Storing/ releasing gas for gas storage.
G_{nt}^Ω	Gas production for a gas well.
π_{nt}^Ω	Gas pressure for a node.
D_{nt}^Ω	Total gas load at a node.
\tilde{D}_{nt}^Ω	Electrical gas load.
$f_{nm,t}^\Omega / f_{nm,t}^\Omega$	Outflow/inflow of a gas pipeline.
E_{nt}^Ω	Gas storage volume for a gas storage.
$\lambda_{nt}^\Omega / \lambda_{nt}^\Omega$	Binary variable to specify storing/releasing gas of a storage.

I. INTRODUCTION

A. Background and motivations

Extreme events involving natural phenomena significantly affect the electrical and energy infrastructure [1]. According to official reports, Hurricane Sandy, when passing through the United States sequentially in 2012, resulted in significant blackouts and financial losses. During Hurricane Sandy, over 8 million customers were left without electricity, and the estimated financial losses in New Jersey and New York exceeded \$70 billion [2]. The majority of the outages caused by the hurricane, about 90%, occurred in electrical distribution systems (EDSs). In the future, the severity and frequency of hurricanes are anticipated to increase significantly as a result of climate change [2]. Thus, it will be more and more critical to develop methods to enhance the resilience of the EDS operation under $N - k$ contingencies considering the high penetration of renewable generation. The most vulnerable section of the power systems in the occurrence of a hurricane is the conventional EDSs because of the large number of components and a close distance to the end user. Indeed, to enhance the resilience of the EDS operation and integrate large-scale renewable energy resources, such as wind energy generation (WEG), there are two groups of potential solutions [3]: (i) reinforcement actions and infrastructure hardening, such as upgrading the lines with stronger materials or building redundant lines and (ii) utilization of the existing distribution system and harnessing the existing flexible resources of the EDS before building new or upgrading old distribution lines. The first option is extremely expensive in terms of costs, can cause dissatisfaction of the people living close by, and requires several months to complete. In fact, only a small number of actions can be taken because of the inadequate response time during extreme hurricane events. Accordingly, a cheaper, faster, and more attractive alternative to the first unattractive option is the more effective utilization of the existing EDS, e.g., harnessing modern tools, such as fast natural gas units (NGUs) and power-to-gas (P2G) technologies. During extreme hurricane events, the volatility and uncertainty behaviors of wind power generations (WPGs) increase significantly. Thus, integration of large-scale WPGs in an EDS without deploying fast NGUs and P2G technologies is an intractable task. In recent years, NGUs have gained significant interest in electrical system operation because of their high ramping capabilities, high-speed start-up, and low carbon emissions and capital cost. The delivery of natural gas to NGUs is “just-in-time” and the most crucial task for the EDS operators [3]. Moreover, another major challenge is that supplying interruptible gas loads including NGUs is a difficult task, particularly in cold seasons [3]. To address these issues, P2G technologies can be used, because they are fast response technologies in the power dispatch and ramping regulation. In addition, P2G can accommodate the fluctuations of the ever-increasing WPG in extreme hurricane events [4]. The P2G technology is a system with the ability to reduce the dependence to buy natural gas from the gas system operator by converting WPG into natural gas and providing power between the EDS and the NGS [5]. In addition, the underground installation of major infrastructures could be less vulnerable to extreme conditions

and natural disasters like thunderstorms, hurricanes and physical attacks. Accordingly, the natural gas pipeline system is traditionally designed as an underground infrastructure.

Hence, co-optimization of both the energy systems is critical for the integration of NGUs and P2G technology in order to enhance the resilience of the EDS operation. These shortcomings motivate us to establish a min–max robust optimization model to resolve these issues.

B. Literature survey and research gaps

Recently, researchers have shown an increasing interest in co-optimization of integrated electricity and natural gas systems under extreme natural disasters [6], [7], [8], and [9]. In [6], a data-based robust optimization method is presented to improve the resilience of the co-operation of electrical transmission and gas networks against sequential extreme weather events, e.g., a hurricane event. In [7], a model for the interactions between electrical and natural gas networks is introduced to attain operational resilience in an electrical transmission system. In [8], a planning algorithm for integrated electrical and natural gas transmission systems is established to improve the electrical transmission system resilience in extreme natural disasters. In [9], a robust co-expansion planning model is proposed to improve the resilience of the integrated gas–electric distribution networks by expansion of distribution feeders and natural gas pipelines and installation of new NGUs.

Also, a considerable amount of literature has been published on resilient electrical distribution systems planning problem. In a study investigating resilience-based distribution network expansion planning problem [10], a resilient distribution network planning problem to coordinate the power line hardening and distributed generation resource allocation has been proposed to enhance the resilience of a distribution system in worst N-k contingencies. Ref. [11] presents a the multi-zone and multi-time, dynamic, and resilient electrical distribution expansion planning framework to expand a distribution network resiliently. Also, in [12], a robust optimal distribution line hardening method coupled with multiple provisional microgrids has been presented to improve the distribution system resilience against worst N-k contingencies. Taken together, these literatures are focused on electrical distribution systems impacts while ignoring other energy delivery systems such as natural gas system. Also, these works mainly focus on distribution network planning or line hardening problems. Nevertheless, operational constraints of the integration of NGU and P2G technology are frequently overlooked when the influence of extreme weather in resilience enhancement of EDS is considered.

Recently, a few studies have addressed the resilience of power networks considering extreme weather conditions, e.g., by applying a stochastic approach (SA) in [13] and [14] and a robust optimization approach (ROA) in [14] and [15]. Also, [16] and [17] provide a literature survey on the SA and ROA in all its variants. In [18] and [19], the optimal application of microgrids as a potential solution in increasing and sustaining the distribution system resilience is formulated as a multi-period two-stage scenario-based stochastic mixed-integer linear programming. A stochastic approach has been developed in [20] to protect distribution networks against flood events in a day-ahead horizon. Flood probability distribution functions are used to generate

several flood scenarios at each substation. In [20], a stochastic planning model for improving the resilience of EDS against natural disaster uncertainty has been proposed. But, the main *disadvantage* of the SA can be named as follows: (i) the SA needs prior knowledge of the probability density function of extreme weather events. In fact, extreme weather disasters have a low probability/high impact, and thus, the concept of “probability” cannot be defined for the most of such disasters. (ii) the SA typically requires the generation of a rather large number of scenarios leading to impractically large executing times, even for reasonably large values of the duality gap. If the number of scenarios is reduced by means of scenario reduction methods, the monetary benefits achieved with SA may be reduced. Taken together, the SA cannot model extreme weather disasters in a resilience operation problem, which inescapably results in a solution inaccuracy. But, in comparison with the SA, the ROA does not rely on the probability density function and only considers the extreme weather disaster scenario for the resilience problems.

The existing literature on the ROA is extensive and focuses particularly on the static set $N - k$ contingency condition in power system operation problems [21], [22], [23], [24], and [25]. For example, in [21], the ROA is used to model static set $N - k$ contingency scenarios in co-operation with integrated electricity and natural gas systems. In [22], the ROA is used to identify the critical and vulnerable components within static set scenarios to ensure the resilient co-operation of the integrated EDS&NGS.

Briefly, based on the above literature survey, there are four *research gaps* in the available literature in the area as follows:

- The impact of the integration of large-scale renewable energy resources (RERs) on resilience has been neglected in these studies.
- Many of the previous studies mainly focus on expansion planning strategies of the integrated electricity and natural gas system [6]–[9], whereas the operational constraints of a NGS for resilience enhancement of the EDS operation have received less attention.
- A considerable body of literature published on the co-optimization of integrated electricity and natural gas systems has only focused on decision-making strategies with a *central system operator*. However, the collaboration between an EDS operator and an NGS operator in a centralized manner requires all the information of both the independent energy systems. Therefore, this issue causes a lot of communication pressure, in addition to which each independent energy system operator’s private data, which are generally considered commercially sensitive, may be revealed. In case of the occurrence of an extreme hurricane, the communication system for the centralized system is more likely to be damaged. Thus, autonomous performance in a decentralized program can enhance the resilience under limited data exchange.
- As mentioned in [21]–[25], the extreme contingency scenarios are based on static set scenarios and ignore the temporal and spatial dynamics of the occurrence of extreme weather and natural disasters.
- Finally, Table 1, briefly, compares contributions of this paper with respect to the existing previous works.

Table 1: Taxonomy of survey of previous studies compare with proposed paper (PP).

Ref	Year	System		Resilience Horizon		Optimization Algorithm		Worst-case Spatial and Temporal Dynamics of Uncertainty Model		Uncertainty Approach	
		NGS	EDS			Decentralized	Centralized			SA	ROA
								Operation	Planning		
[11]	2022	N	Y	N	Y	N	Y	N	N	Y	N
[18]	2021	N	Y	Y	N	N	Y	N	N	Y	N
[9]	2020	Y	Y	N	Y	N	Y	Y	N	N	Y
[20]	2021	N	Y	Y	N	N	Y	N	N	Y	N
[26]	2019	Y	N	Y	N	Y	Y	N	N	N	Y
[12]	2017	N	Y	N	Y	N	Y	Y	N	N	Y
[10]	2016	N	Y	N	Y	N	Y	Y	N	N	Y
[27]	2020	Y	N	Y	N	N	Y	N	N	N	Y
[28]	2018	Y	Y	N	Y	N	Y	Y	N	N	Y
[29]	2022	Y	Y	N	Y	N	Y	N	N	N	Y
[30]	2021	Y	N	N	Y	N	Y	N	N	Y	N
[6]	2020	Y	N	Y	N	N	Y	Y	N	N	Y
PP	--	Y	Y	Y	N	Y	Y	Y	Y	N	Y

Y/N denotes that the subject is/is not considered

C. Contributions and organization

In this paper, an iterative decentralized optimization algorithm is proposed to decompose the centralized co-operation of the integrated EDS&NGS. In this solution method, each energy system operator has an independent decision-making method and coordinates its method with other energy systems in an integrated energy system to reduce the total operational costs and improve the EDS operation resilience. This paper proposes a min–max robust resilience-constrained co-operation problem that can model the spatial and temporal dynamics of extreme natural disasters in order to enhance the resilience of the integrated EDS&NGS. The proposed robust min–max resilience problem cannot be solved directly by an off-the-shelf optimization package. Thus, this study proposes an effective solution strategy based on a column-and-constraints generation (C&CG) algorithm to facilitate the solution process. In comparison with the previous literature, the key contributions of this study are summarized as follows:

- The min–max robust resilience optimization is developed based on worst-case $N - k$ contingencies and worst-case realization of WPG in a co-operation integrated EDS&NGS problem for enhancing the EDS resilience under extreme

hurricane events. In addition, wind power generation variations are modeled with an interval uncertainty dynamic set in the proposed robust optimization.

- In the min–max robust resilience optimization problem, a multi-time- and multi-zone based uncertainty set is used to capture the spatial and temporal dynamics of natural disasters, such as extreme hurricanes.
- A computational algorithm based on a hybrid column-and-constraints generation algorithm and an iterative decentralized co-optimization algorithm is proposed. The algorithm solves the min–max robust resilience-constrained co-operation of the integrated EDS&NGS.

The rest of the paper is organized as follows: Section II describes the extreme hurricanes model. The proposed min–max robust co-operation model is introduced in Section III. The solution algorithm is described in detail in Section IV, and the numerical experiments are analyzed in Section V. Conclusions are given in Section VI.

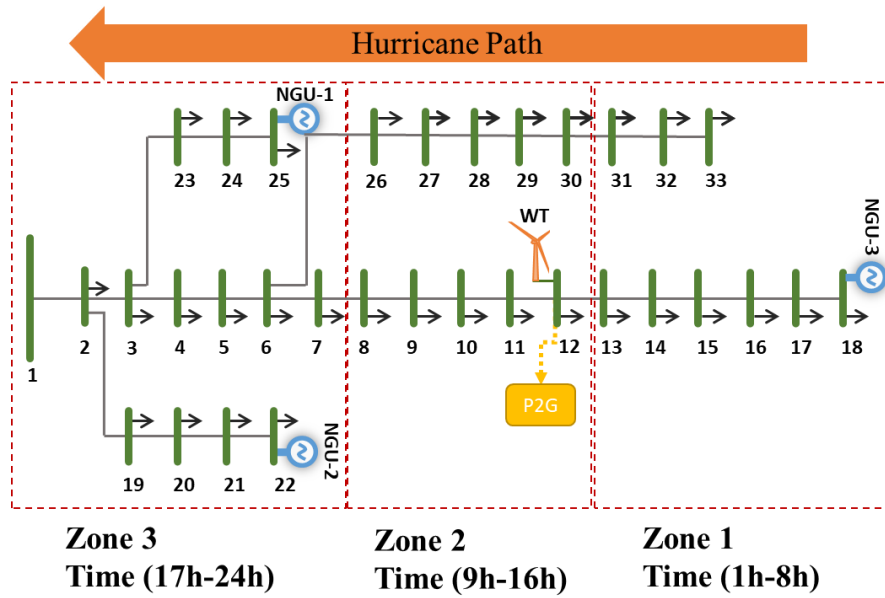


Fig. 1. Multizone and multitime extreme hurricanes model in the IEEE 33-bus.

II. EXTREME HURRICANE MODEL

The proposed multi-zone and multi-time uncertainty set in this study has been considered in order to model the temporal and spatial dynamics of an extreme hurricane event which is a sophisticated uncertainty set but more accurate. Therefore, here, a multi-zone and multi-time natural hurricane event model has been used to extend the conventional $N-k$ contingencies model. To show this idea, the hurricane event is considered as the case of multi-zone and multi-time hurricane event. As mentioned via the Hurricane Forecast Improvement Program [31], a hurricane frequently pass a route that comprises of numerous related multi-zones and multi-times. The most destructive forces of a hurricane relate to the wind speed of a hurricane, which increases when it closes to a zone and reduces when it drifts away from the zone. According to the spatial and temporal dynamics of a

hurricane, in this study is supposed once a hurricane transfers into an area, it will land on the zone that is close to the strong rotating wind will affect the distribution lines within the zone whereas the far-away distribution lines will stay intact. Within the affected zone, in order to estimate impacts of the hurricane on the distribution lines an $N-k$ contingency constraint is applied. Based on the geographic locations, when the hurricane transfers into the inland area, it will cross the areas from one zone to another. A hurricane route in the IEEE 33-bus distribution system is shown by Fig. 1. Firstly, the ADS is divided into three (or more) zones according to the geographic situations of the distribution lines and route of the hurricane movement.

As can be seen in Fig. 1 Zone 1 is close to the hurricane center. Therefore, during the first time period and stage the distribution lines of this zone will damage extremely from the hurricane impact. In the next time, the hurricane will transfer to Zone 2 and the distribution lines in this zone are damaged. Lastly, the hurricane will reach Zone 3 and damage, usually to a less impact and extent, the related distribution lines. Similarly, power generation uncertainty of wind turbine (WT) in this zone are affected by hurricane.

Based on such observations and dynamics, the multi-zone and multi-time hurricane events can be divided into multi-zones and multi-time period according to the hurricane routes. In order to model the hurricane event, the following uncertainty set Ω^c can be implemented, thus, the uncertainty set Ω^c is characterized based on the multi-zone and multi-time period.

$$\Omega^c = \left\{ z_{kt} : \text{Damage lines in Zone1} \left\{ \sum_{k \in \Pi_1} (1 - z_{k,1}) \leq \eta_1 \right\}, \right. \quad (1)$$

$$\left. \text{Undamaged lines except Zone1} \left\{ z_{k,1} = 1, \quad \forall k \in \{\Pi_0 / \Pi_1\} \right\}, \forall t \in \left[1, \mathbf{K}, \frac{T}{Z} \right] \right\} \quad (2)$$

$$\left. \text{Damage lines in Zone 2} \left\{ \sum_{k \in \Pi_2} (1 - z_{k,2}) \leq \eta_2 \right\} \right\} \quad (3)$$

$$\left. \text{Undamaged lines except Zone2} \left\{ z_{k,2} = z_{k,1}, \quad \forall k \in \{\Pi_0 / \Pi_2\} \right\}, \forall t \in \left[\frac{T}{Z} + 1, \mathbf{K}, \frac{2T}{Z} \right] \right\} \quad (4)$$

\mathbf{N}

$$\left. \text{Damage lines in Zone } Z \left\{ \sum_{k \in \Pi_Z} (1 - z_{k,T}) \leq \eta_Z \right\} \right\} \quad (5)$$

$$\left. \text{Undamaged lines except Zone } Z \left\{ z_{k,T} = z_{k,T-1}, \forall k \in \{\Pi_0 / \Pi_Z\} \right\}, \forall t \in \left[\frac{(\nu-1)T}{Z} + 1, \mathbf{K}, \frac{\nu T}{Z} \right], \forall \nu = \{1, \dots, Z\} \right\} \quad (6)$$

where z_{kt} is the binary decision variable that represents whether a distribution line k is on outage (i.e., $z_{kt} = 0$) or not outage

in time period $t \in \left[\frac{(\nu-1)T}{Z} + 1, \mathbf{K}, \frac{\nu T}{Z} \right]$. First thing to remember, parameter Z shows total number of zones, ν signify zone

number. For example, when the ADS is divided into three zones, parameter $Z = 3$, in this condition, zone numbers are $\nu = \{1, 2, 3\}$. Also, parameter T displays length of operation time horizon, for our operation, its value is 24 hours. Parameter

η_ν is the threshold budget for the number of distribution line contingencies in the damaged Zone ν . Also, the length of time period for hurricane event in Zone ν is defined by $\left[\frac{(\nu-1)T}{Z} + 1, \mathbf{K}, \frac{\nu T}{Z} \right]$. In fact, the length of time period is the operation time horizon, i.e., T , is divided into Z according to the speed and route of the hurricane in Zone ν . For instance, constraint (1) denotes that the number of outage distribution lines (i.e., $z_{kt} = 0$) in Zone 1 must not surpass threshold budget η_1 . The set of distribution lines before hurricane event is shown by Π_0 and the set of distribution lines which are not placed in Zone 1 is shown by $\{\Pi_0 / \Pi_1\}$. Constraint (2) shows that if a distribution line is not located in Zone 2, will not be damaged (i.e., $z_{kt} = 1$). Constraint (6) denotes that if the distribution lines are not located in Zone ν , will remain in the same state (on/off) in time period $\left[\frac{(\nu-1)T}{Z} + 1, \mathbf{K}, \frac{\nu T}{Z} \right]$. Based on the multi-zone and multi-time period uncertainty set Ω^c , the impact of hurricane event within each zone is modeled as an extreme $N-k$ contingencies.

The uncertainty relating to the RES, e.g., wind power generation (WPG), is modeled by a bounded interval within the multi-zone and multi-time polyhedral uncertainty set as follows:

$$\Omega^w = \left\{ \begin{array}{l} P_{wt} : |P_{wt} - \bar{P}_{wt}| \leq \hat{P}_{wt} \\ \sum_w \left| \frac{P_{wt} - \bar{P}_{wt}}{\hat{P}_{wt}} \right| \leq \alpha_{zt}, \forall w \in \Psi_\nu, t \in \left[\frac{(\nu-1)T}{Z} + 1, \mathbf{K}, \frac{\nu T}{Z} \right] \end{array} \right\} \quad (7)$$

In (7), the budget of uncertainty α_{zt} is applied to handle the degree of robustness that is modeled based on multi-zone and multi-time period. Further, once α_{zt} decreases/increases, a lower/higher number of wind farms can deviate from their forecast generation values, resulting in a lower/higher degree of robustness. Accordingly, the maximum and minimum values for the budget of uncertainty are 1 and 0, respectively. In this model, when the hurricane moves to Zone ν , the WT located in Zone ν has a maximum value for the $\alpha_{zt}, \forall w \in \Psi_\nu, t \in \left[\frac{(\nu-1)T}{Z} + 1, \mathbf{K}, \frac{\nu T}{Z} \right]$, and when the hurricane moves from Zone ν , or in case of other zones and times, i.e., $\forall w \notin \Psi_\nu, t \notin \left[\frac{(\nu-1)T}{Z} + 1, \mathbf{K}, \frac{\nu T}{Z} \right]$, it (α_{zt}) has a minimum value.

III. PROPOSED MODEL FORMULATION

A. Assumptions

The main assumptions in the model proposed in this paper are as follows:

- The overhead power grids, e.g., distribution lines and WTs, face extreme events, here a hurricane.

- In general, the underground installation of major infrastructures could be less vulnerable to extreme conditions and natural disasters like thunderstorms, hurricanes and physical attacks. Accordingly, the natural gas pipeline system is traditionally designed as an underground infrastructure.

The centralized co-operation of the integrated EDS&NGS problem with the min–max robust resilience-constrained approach is formulated in detail as follows:

B. Problem Formulation

- Objective function

The objective function (8) represents the total operation cost for the EDS operator, Θ^E , and the NGS operator, Θ^N , respectively.

$$\Theta^{TC} = \min(\Theta^E + \Theta^N) \quad (8)$$

The EDS and NGS security constraints are explained in detail as follows:

- EDS Operation Constraints

$$\min \Theta^E = \sum_t \sum_g (c_g P_{gt} + c_g^{su} v_{gt}) + \sum_t (c_t^l P_t^l + c_t^r P_t^r) \quad (9)$$

$$v_{gt} - w_{gt} = u_{gt} - u_{g,t-1} \quad (10)$$

$$\sum_{t'=t}^{t-UT_g+1} u_{g,t'} \leq UT_g v_{gt} \quad (11)$$

$$\sum_{t'=t}^{t-DT_g+1} (1-u_{g,t'}) \leq DT_g w_{gt} \quad (12)$$

$$P_{gt} u_{gt} \leq P_{gt}^\Omega \leq \bar{P}_{gt} u_{gt} : 1^1, 1^2_{gt} \quad (13)$$

$$-\bar{Q}_{gt} u_{gt} \leq Q_{gt}^\Omega \leq \bar{Q}_{gt} u_{gt} : 1^3_{gt}, 1^4_{gt} \quad (14)$$

$$\Delta r_g \leq (P_{gt}^\Omega - P_{g,t-1}^\Omega) \leq \bar{\Delta} r_g : 1^5_{gt}, 1^6_{gt} \quad (15)$$

$$P_{ij,t}^\Omega = g_k (V_{it}^\Omega - V_{jt}^\Omega - \psi_{ij,t}^\Omega + 1) - b_k \varphi_{ij,t}^\Omega : 1^7_{ij,t} \quad (16)$$

$$Q_{ij,t}^\Omega = -b_k (V_{it}^\Omega - V_{jt}^\Omega - \psi_{ij,t}^\Omega + 1) - g_k \varphi_{ij,t}^\Omega : 1^8_{ij,t} \quad (17)$$

$$\psi_{ij,t}^\Omega = \gamma_{ij} \varphi_{ij,t}^\Omega + \lambda_{ij} : 1^9_{ij,t} \quad (18)$$

$$-\bar{\varphi} \leq \varphi_{ij,t}^\Omega \leq \bar{\varphi} : 1^{10}_{ij,t}, 1^{11}_{ij,t} \quad (19)$$

$$-\bar{P}_{ij} z_{kt} \leq \varphi_{ij,t}^\Omega \leq \bar{P}_{ij} z_{kt} : 1^{12}_{ij,t}, 1^{13}_{ij,t} \quad (20)$$

$$-\bar{Q}_{ij} z_{kt} \leq \varphi_{ij,t}^\Omega \leq \bar{Q}_{ij} z_{kt} : 1^{14}_{ij,t}, 1^{15}_{ij,t} \quad (21)$$

$$V_{it} \leq V_{it}^\Omega \leq \bar{V}_{it} : 1^{16}_{it}, 1^{17}_{it} \quad (22)$$

$$P_{ij,t}^\Omega - M(1-z_{kt}) \leq \varphi_{ij,t}^\Omega \leq P_{ij,t}^\Omega + M(1-z_{kt}) : 1^{18}_{ij,t}, 1^{19}_{ij,t} \quad (23)$$

$$Q_{ij,t}^{\Omega} - M(1 - z_{kt}) \leq Q_{ij,t}^{\theta} \leq Q_{ij,t}^{\Omega} + M(1 - z_{kt}) : 1_{ij,t}^{20}, 1_{ij,t}^{21} \quad (24)$$

$$-z_{kt}M \leq P_{ij,t}^{\theta} \leq z_{kt}M : 1_{ij,t}^{22}, 1_{ij,t}^{23} \quad (25)$$

$$-z_{kt}M \leq Q_{ij,t}^{\theta} \leq z_{kt}M : 1_{ij,t}^{24}, 1_{ij,t}^{25} \quad (26)$$

$$-P_t^{\max} \leq P_t^{\Omega} \leq P_t^{\max} : 1_t^{26}, 1_t^{27} \quad (27)$$

$$-Q_t^{\max} \leq Q_t^{\Omega} \leq Q_t^{\max} : 1_t^{28}, 1_t^{29} \quad (28)$$

$$\sum_g P_{gt}^{\Omega} + \sum_w P_{wt}^{\Omega} + P_t^{\Omega} - \sum_{ij} P_{ij,t}^{\theta} = P_{it} + \sum_v P_{vt}^{\Omega} \quad (29)$$

$$\sum_g Q_{gt}^{\Omega} + Q_t^{\Omega} - \sum_{ij} Q_{ij,t}^{\theta} = Q_{it} \quad (30)$$

The objective function of the EDS is shown by the equality constraint (9), which includes the generation cost (first term) and the start-up cost (second term) for a distribution generator (DG) and the purchase (or sales) cost of the active power from/to the transmission network (third term), respectively. Note that constraints (10)–(30) are related to before the realization of the hurricane or the worst-case $N - k$ contingencies (labeled as the base case constraints). The on (start-up)/off (shutdown) states of a DG are denoted by (10). Constraints (11) and (12) represent the minimum on/off time limits for a DG. Constraints (13) and (14) enforce the active and reactive power generations for a DG. Constraint (15) limits the ramp down/up for a DG. Finally, constraints (16)–(18) represent linearized AC optimal power flow (L-ACOPF) constraints.

It should be noted that further explaining the details of the linearization method in order to linearize the nonlinear AC optimal power flow (ACOPF) constraints is not the main concern of this study. Hence, for full details of the linearization method for these linear constraints, the reader is referred to [32]. Constraint (18) defines a linear estimate for the nonlinear cosine term of the L-ACOPF constraints (16)–(17). In this regard, the variable $\psi_{ij,t}$ in (18) denotes the cosine value (i.e., $\cos \psi_{ij,t}^{\Omega}$) for the bus voltage angle through line ij . Constraint (19) shows the min/max voltage angle across a distribution line. The disjunctive constraints (23) and (24) denote the min and max active and reactive power flows through a distribution line, which are used to avoid the nonlinearity that would otherwise appear. The active/reactive power flow on each distribution line is enforced to be zero through (25) and (26) when there is a distribution line outage. In fact, the binary variable z_{kt} within (23)–(26) enforces the flow of the distribution line to be zero once there is a distribution line outage. Similarly, in (23)–(26), M is termed as the “big M ” value, where M is large enough to make these constraints nonbinding. Note that before the realization of the hurricane or the worst-case $N - k$ contingencies, the binary variable z_{kt} in constraints (20)–(21) and (23)–(26) is 1. The active and reactive powers sold to and bought from a substation are limited by (27) and (28), respectively. Constraints (29) and (30) ensure the balance of active and reactive power at each bus.

- *NGS Operation Constraints*

$$\min \Phi^N = \sum_t \sum_n \left(\nu_n G_{nt}^\Omega + \mathcal{G}_n \left(S_{nt}^{\mathbf{r}\Omega} + S_{nt}^{\mathbf{s}\Omega} \right) + \zeta_n \bar{D}_{nt}^\Omega \right) \quad (31)$$

$$\underline{G}_n \leq G_{nt}^\Omega \leq \bar{G}_n \quad (32)$$

$$\underline{\pi}_n \leq \pi_{nt}^\Omega \leq \bar{\pi}_n \quad (33)$$

$$D_{nt}^\Omega = \tilde{D}_{nt}^\Omega + \bar{D}_{nt} - \bar{D}_{nt}^\Omega \quad (34)$$

$$0 \leq \bar{D}_{nt}^\Omega \leq D_{nt}^\Omega \quad (35)$$

$$\bar{D}_{nt}^\Omega = \eta_{NGU} \bar{P}_{nt}^\Omega, \forall g(i) \in n \quad (36)$$

$$\begin{aligned} & \left[f_{nm,t+1}^{\mathbf{s}\Omega} + f_{nm,t+1}^{\mathbf{r}\Omega} - f_{nm,t}^{\mathbf{s}\Omega} - f_{nm,t}^{\mathbf{r}\Omega} \right] + \\ & \Upsilon_{nm} \Delta t \left[f_{nm,t+1}^{\mathbf{s}\Omega} + f_{nm,t+1}^{\mathbf{r}\Omega} + f_{nm,t}^{\mathbf{s}\Omega} + f_{nm,t}^{\mathbf{r}\Omega} \right] + \end{aligned} \quad (37)$$

$$\frac{\Delta t}{L_{nm}} \left[\pi_{n,t+1}^\Omega - \pi_{m,t+1}^\Omega + \pi_{n,t}^\Omega - \pi_{m,t}^\Omega \right] = 0$$

$$\begin{aligned} & \mathcal{K}_{nm} \Delta t \left[f_{nm,t+1}^{\mathbf{s}\Omega} - f_{nm,t+1}^{\mathbf{r}\Omega} + f_{nm,t}^{\mathbf{s}\Omega} - f_{nm,t}^{\mathbf{r}\Omega} \right] + \\ & \left[\pi_{n,t+1}^\Omega - \pi_{m,t+1}^\Omega + \pi_{n,t}^\Omega - \pi_{m,t}^\Omega \right] = 0 \end{aligned} \quad (38)$$

$$E_{nt}^\Omega - E_{n,t-\Delta t}^\Omega = \Delta t \left[S_{nt}^{\mathbf{r}\Omega} - S_{nt}^{\mathbf{s}\Omega} \right] \quad (39)$$

$$\underline{E}_n \leq E_{nt}^\Omega \leq \bar{E}_n \quad (40)$$

$$\underline{S}_n \lambda_{nt}^{\mathbf{r}\Omega} \leq S_{nt}^{\mathbf{r}\Omega} \leq \bar{S}_n \lambda_{nt}^{\mathbf{r}\Omega} \quad (41)$$

$$\underline{S}_n \lambda_{nt}^{\mathbf{s}\Omega} \leq S_{nt}^{\mathbf{s}\Omega} \leq \bar{S}_n \lambda_{nt}^{\mathbf{s}\Omega} \quad (42)$$

$$\lambda_{nt}^{\mathbf{r}\Omega} + \lambda_{nt}^{\mathbf{s}\Omega} \leq 1 \quad (43)$$

$$\begin{aligned} & \sum_n \left(\bar{S}_{nt}^\Omega - \tilde{S}_{nt}^\Omega \right) + \sum_{p(n,m)} \bar{f}_{nm,t}^\Omega \\ & - \sum_{p(n,m)} \tilde{f}_{nm,t}^\Omega + \sum_n G_{nt}^\Omega + \sum_{v(n) \in n} \eta_{P2G} \bar{P}_{vt}^\Omega = D_{nt}^\Omega \end{aligned} \quad (44)$$

$$P_{gt}^\Omega = \bar{P}_{gt}^\Omega \quad (45)$$

$$P_{vt}^\Omega = \bar{P}_{vt}^\Omega \quad (46)$$

Like the EDS, the objective function of the NGS is shown by (31), which includes three main terms: the first term, the cost for natural gas well outputs, the second term, the operation cost of charging/discharging processes of the natural gas storage (NGS), and the third term, the cost of unserved natural gas loads. Note that the cost of unserved natural gas demand for nonelectrical gas loads is much higher than that of electrical gas loads. Constraints related to NGS operation are defined by (32)–(46).

Constraints (32) and (33) are the limits on natural gas well outputs and gas pressure, respectively. Constraint (34) shows the total natural gas load, D_{nt}^Ω , which includes three terms: electric load, i.e., NGUs, \bar{D}_{nt}^Ω ; nonelectric load (residential/ industrial load), \bar{D}_{nt} ; and unserved gas load, \bar{D}_{nt}^Ω . Constraint (35) is the limit on unserved natural gas load. The natural gas consumption

of the electric load, i.e., the NGU, is expressed by constraint (36). Unlike the electric power flows, which are transferred practically immediately from the generator units to the demand, the natural gas flows more slowly from a natural gas well to gas loads, which causes an inherent gas pipeline pack effect, which is similar to spinning reserves in an EDS. However, previous studies have typically focused on the steady-state model of gas flow, whereas the transient-state model of gas flow has often been neglected. Thus, based on [26], a linear transient-state model is implemented in this study to model the gas pipeline pack effect in an NGS operation problem. Further details of the linearized approximation procedure and formulation of the transient-state model of gas flow are given in [26]. The natural gas flow through a pipeline based on the Wendroff Difference approximation [26] is expressed by (37). The transient-state constraint in natural gas pipelines based on the Wendroff Difference approximation is given by (38). The state of charge (SOC) of the NGS is described by (39) and (40). Constraints (41)–(43) are the limits on the stored natural gas capacity, natural gas inflow, and outflow for each NGS, respectively. In the natural gas system, the natural gas may flow into the NGS or out from the NGS, or it may be idled, which is denoted by (43). Constraint (44) represents a gas nodal balance, which expresses that the gas outflows and inflows are equal at all of the natural gas nodes. Constraints (45)–(46) are coupling constraints and include coupling set variables, $\{P_{gt}^\Omega, P_{vt}^\Omega\}$ and $\{\bar{P}_{gt}^\Omega, \bar{P}_{vt}^\Omega\}$, which couple both the energy systems. In fact, the NGUs, \bar{P}_{gt}^Ω , and the P2G system, \bar{P}_{vt}^Ω , are connected to an EDS and are usually modeled as a gas load and a gas source on the NGS side, respectively, and also as an electrical source, P_{gt}^Ω , and an electrical load, P_{vt}^Ω , on the EDS side.

- *Finding the extreme hurricane events*

$$\max_{\Xi_1} \min_{\Xi_2} \sum_r \sum_t (\Delta P_{it}^r + \Delta Q_{it}^r) \quad (47)$$

$$(13) - (28), \forall \Omega \in \{r\} \quad (48)$$

$$\begin{aligned} \sum_g P_{gt}^r + \sum_w P_{wt}^r + P_t^r \\ - \sum_{ij} P_{ij,t}^r = P_{it} + \sum_v P_{vt}^r - \Delta P_{it}^r : 1_{it}^{30} \end{aligned} \quad (49)$$

$$\sum_g Q_{gt}^r + Q_t^r - \sum_{ij} Q_{ij,t}^r = Q_{it} - \Delta Q_{it}^r : 1_{it}^{31} \quad (50)$$

$$0 \leq \Delta P_{it}^r \leq P_{it} : 1_{it}^{33} \quad (51)$$

$$0 \leq \Delta Q_{it}^r \leq Q_{it} : 1_{it}^{34} \quad (52)$$

$$0 \leq P_{vt}^r \leq \bar{P}_{vt} : 1_{vt}^{35} \quad (53)$$

$$\Omega^c = \{(1) - (6)\} \text{ and } \Omega^W = \{(7)\} \quad (54)$$

where $\Xi_1 = \{P_{wt}^r, z_{kt}\}$, and $\Xi_2 = \{P_{gt}^r, Q_{gt}^r, \tilde{P}_t^r, \tilde{Q}_t^r, \tilde{P}_{ij,t}^r, \tilde{Q}_{ij,t}^r, P_{ij,t}^r, Q_{ij,t}^r, V_{i,t}^r, \psi_{ij,t}^r, \varphi_{ij,t}^r\}$. The aim of the max–min robust problem (47)–(54) is to identify the extreme hurricane events that involve worst-case $N - k$ contingencies. The max–min objective function (47) represents the total cost of the electrical load that is unserved at each bus to avoid problem infeasibility. The objective function (47) has outer maximization and inner minimization processes; the outer maximization process represents the extreme consequence of possibly severe events, e.g., worst-case $N - k$ contingencies and worst-case wind power uncertainty, whereas the inner minimization process is related to the EDS operation actions to modify the effects of such severe events. The related EDS operation constraints, i.e., (13)–(28) in (48), were discussed above, but these constraints are related to the severe condition operation, i.e., extreme hurricane events. Constraints (49) and (50) are like (29) and (30) but include the unserved electrical active and reactive loads, $\{\Delta P_{nt}^r, \Delta Q_{nt}^r\}$, respectively. The maximum values of unserved active and reactive loads are limited by (51) and (52), respectively. Constraints (1)–(7) are discussed in Section II.

Important to realize, the problem (47)–(54) is an adaptive robust max–min model, which is well-known model for optimization problems in engineering sciences. In fact, the robust max–min model is a general model and a considerable amount of literature in power system optimization problems have been used this robust model, e.g., [10], [12] and [33]. Also, formally prove global convergence in mathematical approach for the mentioned robust model is a difficult task which is beyond the scope of these papers and it needs a separate paper.

IV. PROPOSED SOLUTION ALGORITHM

In this section, a three-level hierarchical method, as an effective decentralized solution strategy, is proposed to solve the min–max robust resilience-constrained co-operation of the integrated EDS&NGS. In fact, the proposed hierarchical optimization method includes three levels as shown in Fig. 2:

- The first level is related to the EDS operation problem under worst-case $N - k$ contingencies and extreme wind power uncertainty conditions;
- The second level is related to the NGS operation problem;
- The third level is related to a max–min robust resilience-constrained optimization problem for identifying the multi-time and multi-zone based uncertainty set caused by extreme hurricane events, i.e., worst-case $N - k$ contingencies and extreme wind power uncertainty.

The following parts describe the details of the proposed three-level hierarchical method.

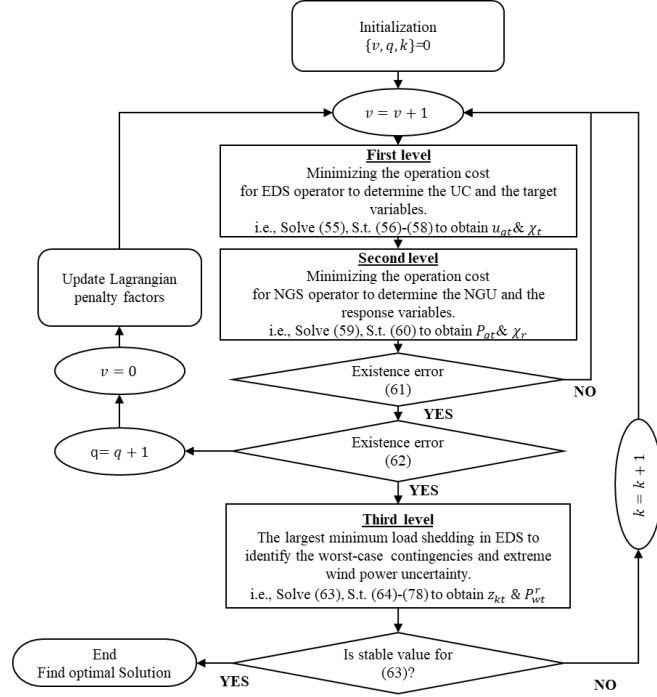


Fig. 2. Tri-level algorithm to solve the max–min robust resilience-constrained co-optimization model.

A. Interactions between First and Second Levels

As mentioned above, the centralized decision-making strategy for co-operation of integrated EDS&NGS is not applicable in the real world because the EDS&NGS are operated independently through an EDS operator and an NGS operator. Therefore, to have a completely decentralized operation, the collaboration between the first and second levels is essential, and thus, an independent two-level hierarchical method is proposed. In fact, the independent two-level hierarchical method decomposes the co-operation of the integrated EDS&NGS into two independent operation problems. The EDS operation problem is located at the upper level (first level) and the NGS operation problem at the lower level (second level). Further, the two-level hierarchical method uses two main sets of target and response variables to model the shared information in the decentralized decision-making strategy. The sets of target variables are defined by $\chi_t \in \{P_{gt}^\Omega, P_{vt}^\Omega\}$ in the EDS operation problem, and the sets of response variables are represented by $\chi_r \in \{\bar{P}_{gt}^\Omega, \bar{P}_{vt}^\Omega\}$ in the NGS operation problem as vectors of shared information provided by the collaborating operators. The proposed solution method finds an optimal solution if the consistency constraint $\chi_t - \chi_r = 0$ is satisfied by the decentralized collaboration.

First level (the EDS operation problem): The mathematical model of the EDS operation problem can be written as follows:

$$\min \Theta^F + c^u (\Delta P_{ii}^r + \Delta Q_{ii}^r) + \tau (\chi_i - \hat{\chi}_i) + \bar{\tau} \|\chi_i - \hat{\chi}_i\|_2^2 \quad (55)$$

$$(10)-(12) \quad (56)$$

$$(13)–(30) \forall \Omega \in \{o\} \quad (57)$$

$$(13)–(30) \forall \Omega \in \{r\} \quad (58)$$

In this part, the objective function (55) has three key terms; the first is the same as (9) described in Section III. The next term shows the cost of unserved active and reactive loads under severe hurricane conditions. The last term is related to the penalty function that defines the shared sets of response variables. Note that in the third term, the set of target variables, χ_t , is determined by the EDS operation problem, whereas the set of response variables, $\hat{\chi}_r$, is determined by the NGS operation problem. Note that $\hat{\chi}_r$ in (55) is a constant value determined by the NGS operation problem.

Further, the EDS operator is coordinated by the NGS operator through a set of response variables, $\hat{\chi}_r$, in the penalty functions. Note that the parameters τ and $\bar{\tau}$ in the penalty function are Lagrangian penalty terms, which are updated through an iterative solution procedure. The penalty functions include two parts: linear and quadratic. A critical feature of the quadratic term, $\bar{\tau} \|\chi_t - \hat{\chi}_r\|_2^2$, is that it is a convex second-order curve. Hence, the quadratic part can be linearized based on [34]. Meanwhile, the EDS operation constraints (56)–(58) should be satisfied. Note that, constraint (58) includes unit commitment and network reconfiguration decisions for both before and after the extreme hurricane event. Similarly, constraints (57) and (58), respectively, are related to operation constraints before and after the extreme hurricane event. It should be noted that the variables in (57) and (58) with $\Omega \in \{o\}$ and $\Omega \in \{r\}$ superscripts are related to before and after the extreme hurricane event, respectively.

Second level (the NGS operation problem): The mathematical model of the stochastic NGS operation is presented by:

$$\text{Min } \Phi^N + \tau(\chi_r - \hat{\chi}_r) + \bar{\tau} \|\chi_r - \hat{\chi}_r\|_2^2 \quad (59)$$

$$(32)–(44) \quad (60)$$

Like (55), the objective function (59) comprises two principal terms, the first term and (31), similar to as described in Section III. The next term defines the penalty function, which is a shared set of target variables, $\hat{\chi}_t$. In the second term, the set of target variables, $\hat{\chi}_t$, is a fixed parameter, which is determined by the EDS operation problem, and hence, the set of response variables χ_r should be determined by the NGS operation problem. Meanwhile, the NGS operation constraints (32)–(44) in (60) were explained in detail in the previous section.

Convergence strategy: The set of target and response variables χ_t and χ_r is shared information that is transferred between EDS&NGS operation problems, and an iterative procedure between first- and second-level operation problems continues until the following stopping criteria are satisfied:

$$\begin{cases} \left| \chi_t^v - \chi_t^{(v-1)} \right| \leq \varepsilon \\ \left| \chi_r^v - \chi_r^{(v-1)} \right| \leq \varepsilon \end{cases} \quad (61)$$

$$\left| \chi_t^g - \chi_r^g \right| \leq \varepsilon \quad (62)$$

where ε is the prespecified error level; the subscript ν shows iterative calculation between the EDS&NGS operation problems. Noted that, the optimal solution and global convergence for first- and second-level operation problems are obtained if the continues target and response variables, i.e. χ_t and χ_r , at iteration “ q ” become identical.

Third level (Identifying the worst-case $N - k$ contingencies and extreme wind power uncertainty): At this level, the max–min robust resilience-constrained optimization problem, i.e., constraints (47)–(54) should be solved to identify the multi-zone and multi-time extreme uncertainty realizations, i.e., the worst-case $N - k$ contingencies and extreme wind uncertainty. However, this max–min robust optimization problem cannot be solved directly by the existing commercial solvers. Hence, in this section, the max–min robust problem based on dual theory is converted into a maximizing optimization problem, i.e., constraints (63)–(78), which can solve this problem with existing solving tools. Point often overlooked, for converting max-min model to a max-max model, the objective functions must be a mixed-integer linear equation or a linear equation, otherwise the max-min model cannot be converted to a max-max optimization model by the strong duality theory, in this condition, may be happen saddle point problem for max-min optimization model [35]. The formulation of the maximizing optimization problem is explained in detail as follows:

$$\begin{aligned}
& Max \sum_t \sum_g (P_g \hat{u}_{gt}^1 1_{gt}^1 - \bar{P}_g \hat{u}_{gt}^1 1_{gt}^2) - \sum_t \sum_g (\bar{Q}_g \hat{u}_{gt}^1 1_{gt}^3 + \bar{Q}_g \hat{u}_{gt}^1 1_{gt}^4) \\
& + \sum_t \sum_g (\underline{\Delta} r_g 1_{gt}^5 - \bar{\Delta} r_g 1_{gt}^6) + \sum_t \sum_{ij} (g_k 1_{ij,t}^7 - b_k 1_{ij,t}^8) \\
& + \sum_t \sum_{ij} \lambda_{ij} 1_{ij,t}^9 - \bar{\varphi} \sum_t \sum_{ij} (1_{ij,t}^{11} + 1_{ij,t}^{10}) \\
& - \sum_t \sum_{ij} z_{kt} (\bar{P}_{ij} (1_{ij,t}^{12} + 1_{ij,t}^{13}) + \bar{Q}_{ij} (1_{ij,t}^{14} + 1_{ij,t}^{15})) \\
& - M \sum_t \sum_{ij} (1 - z_{kt}) ((1_{ij,t}^{18} + 1_{ij,t}^{19}) + (1_{ij,t}^{20} + 1_{ij,t}^{21})) \\
& M \sum_t \sum_{ij} z_{kt} ((1_{ij,t}^{22} + 1_{ij,t}^{23}) - (1_{ij,t}^{24} + 1_{ij,t}^{25})) \\
& - M \sum_t \sum_{ij} z_{kt} - \sum_t \sum_v \bar{P}_{vt} 1_{vt}^{35} \\
& + \sum_t (P_t^{\max} (1_t^{26} - 1_t^{27}) + Q_t^{\max} (1_t^{28} - 1_t^{29})) \\
& + \sum_t \sum_i (P_{it} 1_{it}^{30} + Q_{it} 1_{it}^{31}) + \sum_t \sum_w P_{wt}^r 1_{it}^{30} \\
& - \sum_t \sum_i (P_{it} 1_{it}^{33} + Q_{it} 1_{it}^{34}) + \sum_t \sum_i (V_{-i} 1_{it}^{16} - V_{-i} 1_{it}^{17})
\end{aligned} \tag{63}$$

$$1_{gt}^1 - 1_{gt}^2 + 1_{gt}^5 - 1_{gt}^6 - 1_{g,t-1}^5 + 1_{g,t-1}^6 + 1_{it}^{30} \leq 0 \tag{64}$$

$$1_{gt}^3 - 1_{gt}^4 + 1_{it}^{31} = 0 \tag{65}$$

$$1_{ij,t}^7 - 1_{ij,t}^{18} + 1_{ij,t}^{19} = 0 \tag{66}$$

$$1_{ij,t}^8 - 1_{ij,t}^{20} + 1_{ij,t}^{21} = 0 \tag{67}$$

$$\begin{aligned}
& \sum_{ij} g_k (1_{ji,t}^7 - 1_{ij,t}^7) + \sum_{ij} b_k (1_{ij,t}^8 - 1_{ji,t}^8) \\
& + 1_{ij,t}^{16} - 1_{ij,t}^{17} \leq 0
\end{aligned} \tag{68}$$

$$g_k 1_{ij,t}^7 - b_k 1_{ij,t}^8 + 1_{ij,t}^9 \leq 0 \quad (69)$$

$$b_k 1_{ij,t}^7 + g_k 1_{ij,t}^8 - \gamma_{ij} 1_{ij,t}^{19} + 1_{ij,t}^{10} - 1_{ij,t}^{11} = 0 \quad (70)$$

$$1_{ij,t}^{12} - 1_{ij,t}^{13} + 1_{ij,t}^{18} - 1_{ij,t}^{19} + 1_{ij,t}^{22} - 1_{ij,t}^{23} - 1_{it}^{30} = 0 \quad (71)$$

$$1_{ij,t}^{14} - 1_{ij,t}^{15} + 1_{ij,t}^{20} - 1_{ij,t}^{21} + 1_{ij,t}^{24} - 1_{ij,t}^{25} - 1_{it}^{31} = 0 \quad (72)$$

$$1_t^{26} - 1_t^{27} + 1_t^{30} = 0 \quad (73)$$

$$1_t^{28} - 1_t^{29} + 1_t^{31} = 0 \quad (74)$$

$$1_{it}^{30} - 1_{it}^{33} \leq 1 \quad (75)$$

$$1_{it}^{31} - 1_{it}^{34} \leq 1 \quad (76)$$

$$-1_{it}^{30} - 1_{vt}^{35} \leq 0 \quad (77)$$

$$\alpha^c = \{(1)-(6)\} \text{ and } \alpha^W = \{(7)\} \quad (78)$$

Equation (63) defines the dual objective function for the dual optimization problem. However, because the binary and continuous variables are multiplied in continuous variables in the objective function (63), $z_{kt} \ell_{(c)}^{(c)}$ and $P_{wt}^r \ell_{it}^{30}$, the dual optimization problem is converted into an MINLP problem, which, as mentioned above, is very problematic to solve. However, the multiplication of the binary and continuous variables in the continuous variables can be linearized by the method proposed in [36]. Thus, the proposed dual optimization problem can easily become a mixed-integer linear programming (MILP) case. Constraints (64)–(77) are associated with the variables $\{P_{gt}^\Omega, Q_{gt}^\Omega, P_{ij,t}^\Omega, Q_{ij,t}^\Omega, V_{i,t}^\Omega, \psi_{ij,t}^\Omega, \varphi_{ij,t}^\Omega, \bar{P}_{ij,t}^\Omega, \bar{Q}_{ij,t}^\Omega, \bar{P}_t^\Omega, \bar{Q}_t^\Omega, \Delta P_{it}^\Omega, \Delta Q_{it}^\Omega\}$, $\forall \Omega \in \{r\}$, respectively. Constraints (64)–(77) are also explained above. Also, constraint (78) has been explained in detail previously. Finally, Fig. 2 summarizes the proposed decentralized solution of the co-operation of the EDS&NGS under extreme uncertainty realizations. More details about the single equivalent dual problem is described in the Appendix.

B. convergence of the proposed solution technique

The convergence of the proposed iterative solution technique can be proved theoretically. Recently, researchers have shown an increased interest in implementing iterative solution strategies in optimization problems [26], [37] and [38]. References [26], [37], and [38] provide an overview of the convergence properties of iterative solution strategies. The following conditions guarantee the convergence of proposed iterative solution strategies: (i) Convexity of EDS and NGS objective functions, (ii) Convexity of EDS and NGS operation constraints, and (iii) Convexity of the max–min robust resilience-constrained optimization problem. Thereby, the convergence property of proposed solution strategy can be guaranteed. Also, the proposed iterative solution strategy has been deployed by the analytical target cascading (ATC) method whose convergence properties are discussed in [34] and [39]. The detailed proof of convergence of ATC has been shown by [39]. The ATC has proved to converge for a convex problem. The EDS and NGS operation constraints and max–min robust resilience-constrained

optimization formulations in our proposed problem are all MILP and convex. Thus, the convergence property of the iterative solution technique deployed to the proposed problem can be guaranteed and an optimal solution of the decentralized model can be provided when the hierarchical optimization process converges. Also, the augmented Lagrangian penalty function, i.e., $\{(\mathcal{Z}_i - \hat{\mathcal{Z}}_i), \|\mathcal{Z}_i - \hat{\mathcal{Z}}_i\|\}$, in the objective functions (54) and (58) and the multiplier, i.e., $\{\tau, \bar{\tau}\}$, are updated which can meaningfully improve the convergence property of the entire optimization problem. Indeed, as a local convexification approach, quadratic penalty terms are added to the objective functions to improve the convexity of the problem [34]. Through an experiment, the effectiveness of the penalty function method has been validated through many experiments, which can usually at least provide a local optimal solution after convergence [40].

Noted that, the mixed-integer linear programming (MILP) is a well-known model in real-world optimization problems. Also, the most literature in power system area have used MILP, because, the MILP combines the integer and linear constraints into a versatile modeling framework. The MILP is often considered as a “difficult” or “non-convex” class of optimization problems. However, there has been significant progress in the field commercial solvers during last twenty years and there are several good solvers for MILP problems available today e.g., CPLEX, BARON, GUROBI, LINDO and XPRESS. Note that all available solvers are, in theory and practical perspectives, capable of finding globally optimal solutions with proven optimality for mixed-integer programming models. In fact, some these solvers convert the MILP problem to a convex problem. As mentioned before, the MILP problems include the integer and linear constraints, the linear constraints are convex, but the integer constraints make original optimization problems to a non-convex problem. Accordingly, in these solvers have replaced a integer constraint with relaxed linear constraint by defining the discrete variable as continuous variable in a integer constraint and it bounded by the original discrete bound. The original optimization problem with continuous relaxation of constraint is a convex problem, thus, it has the global convergence with optimum solution results. If all relaxed integer variables take on integer values, then it is also an optimal solution for the MILP problem. Otherwise, the mentioned solvers use Branch and Bound, Cutting-Plane, Branch and Cut methods or similar methods. Must be remembered, in the Branch and Bound, Cutting-Plane and Branch&Cut methods the non-convex integer inequality constraints are relaxed as convex continuous inequality constraints using relaxed integer variables with continuous variables. When all relaxed integer variables take on integer values, and all equality/non-equality constraints were satisfied then it is also the global convergence and optimal solution for the mentioned solvers.

V. CASE STUDIES

In this study, a modified IEEE 33-bus distribution system with a ten-node natural gas system has been implemented to demonstrate the effectiveness of the proposed model for managing the multi-zone and multi-time worst-case uncertainties in the co-operation of an integrated EDS&NGS problem. The integrated IEEE 33-bus distribution and 10-node natural gas systems are presented in Figs. 1 and 3. The bus connected to the upstream grid is Bus 1, and it has a fixed voltage magnitude

in the EDS. The 33-bus distribution system comprises three NGUs, one wind turbine (WT), P2G technology, 32 distribution lines, and 32 loads. Three NGUs, the WT, and the P2G technology are located at buses [18, 22, 25, 12, 12], which are indicated by G1–G3, WT, and P2G, respectively. The topology of a ten-node gas system is given in Fig. 3, which has ten nodes, ten pipelines, six natural gas loads, and two natural gas suppliers or gas wells, one gas storage and one P2G facility. Furthermore, the locations of the WT, the NGUs, the distribution lines, the P2G facility, the gas wells, the gas storage systems, and the gas pipelines for the 33-bus EDS and 10-node NGS are shown in Figs. 1 and 3. Additional data of the parameters for the EDS and NGS can be found at <http://motor.ece.iit.edu/data/33-bus-6-node.xlsx>. The penalty prices for unserved electrical and gas loads are fixed at 10,000\$/MWh and 100\$/kcf, respectively. The primary penalty multipliers values are fixed at 1, and the prespecified error level for the convergence is set at 0.0001. As shown in Fig. 1, the multi-zone and multi-time dynamic progress process of the extreme hurricane is shown by the IEEE 33-bus distribution system, which is divided into three zones and time periods. Through each zone and period, the hurricane event causes distribution line outages with a pre-defined budget. Note that the distribution lines that experience an outage in the prior zone and time remain in outage in the next zone and period. The proposed solution method was implemented by the solving tools (12.6 CPLEX) in the GAMS software [41] on a computer with an Intel Core i7-4.50 GHz CPU and 16 GB of memory.

This paper considers three different optimization methods for the integrated EDS&NGS:

Isolated method: In this method, the operation problem for the EDS problem (first level) for objective function (9) subject to (10)-(30) and the third level operation problem (identifying the worst-case $N - k$ contingencies and extreme wind power uncertainty) for (63) subject to (64)-(77) and finally the second level operation problem for (31) subject to (32)-(44) are optimized, respectively. Precisely, the first level and third level problems are hierarchically optimized and then the problem formulation of the NGS operation problem is solved by fixing the sets of target variables ($\chi_t \in \{P_{gt}^\Omega, P_{vt}^\Omega\}$) obtained from the first level operation problem.

Decentralized method: This is a hierarchically coordinated method as described in detail in Section IV.

Centralized method: In this method, the original first and second operation level problems for the EDS and NGS in Section III are solved in a joint manner. In fact, the objective function (8) is minimized subject to the EDS operation constraints, i.e., (10)-(30), and the NGS operation constraints, i.e., (32)-(46). The centralized method can achieve an optimal solution, but cannot be implemented in practice, since the EDS and NGS operation problems are executed by different operators. Thus, solution results from this method are only deployed to check the validity of the convergence of the proposed decentralized method.

A. Effectiveness of Hurricane Event

In the proposed min–max robust resilience-constrained co-optimization model, the set \square is defined for hurricane events, the worst-case $N - k$ contingencies, and the worst realizations of wind power uncertainty based on the uncertainty. As shown in

Fig. 1, the IEEE 33-bus distribution system based on the multi-zone and multi-time extreme hurricane model is divided into three zones, including Zones 1, 2, and 3. The total operation period, considered to be 24 h, is divided into three time periods: 1h–8h, 9h–16h, and 17h–24h. It is worthwhile to note that the extreme hurricane crosses a zone during a time period, and thus, as shown in Fig. 1, the time periods 1h–8h, 9h–16h, and 17h–24h are related to the crossing of the hurricane from Zone 1, 2, and 3, respectively.

A set of the budgets of wind uncertainty $\alpha_t = 0.8, \forall t \in [8h, 16h]$, $\alpha_t = 0, \forall t \notin [8h, 16h]$ and worst-case $N - 3$ contingencies ($\eta_1 = \eta_2 = \eta_3 = 1$) is shown by Fig. 1 to demonstrate the proposed multi-zone and multi-time extreme hurricane model. Therefore, the uncertainty associated with wind generators is only considered for a period of 8 h. Similarly, it is apparent from Fig. 1 that there is one distribution line outage at most in each zone and time. For example, in the first time, 1 h–8 h, once the hurricane crosses Zone 1, the distribution line 13–14 is damaged. In the second period, 9 h–16 h, the hurricane moves along its path and damages distribution lines 10–11 in Zone 2. Likewise, in this period, power generation deviations from the nominal power forecasts are considered for the wind turbine installed in Zone 2, i.e., $\alpha_t = 0.8$. Consequently, in the third period, 17h–24h, once the hurricane arrives in Zone 3, it damages distribution lines 3–23. These outages cause 10.08 MW electrical load curtailment (ELC) and 31.64 kcf gas load curtailment (GLC), respectively. The electrical and gas load curtailment and total electrical operation cost (EOC) and the gas operation cost (GOC) for different worst-case $N - k$ contingencies are listed in Table 2. It is interesting that the ELC is significantly increased with an increase in the number of worst-case contingencies in all contingencies.

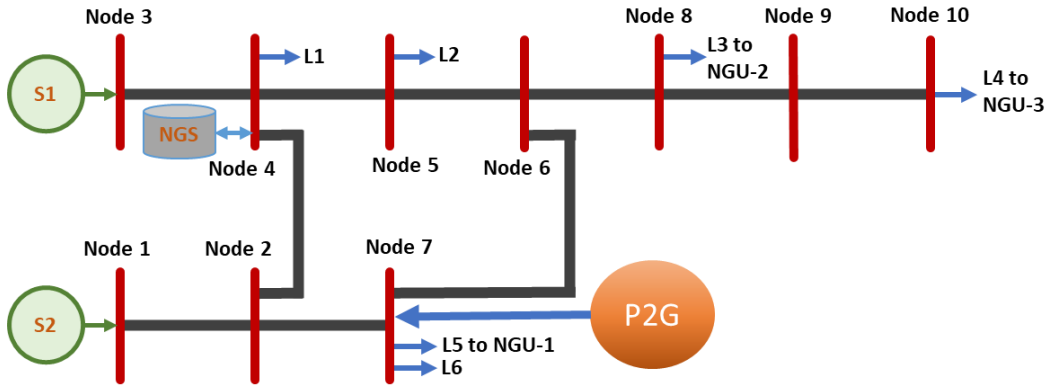


Fig. 3. Topology of a ten-node gas system.

Table 2: Comparison of results for different $N - k$ contingencies; without P2G technology

$N-k$	EOC [M\$]	GOC [k\$]	ELC [MW]	GLC [kcf]	Computational burden [s]
3	1.17	1.02	10.08	31.64	100
4	1.83	1.32	21.05	51.45	133
5	2.08	1.66	89.26	101.15	167

B. Influence of P2G technology

Here, the beneficial role of the P2G facilities in co-operation with the EDS&NGS in the occurrence of an extreme hurricane is analyzed. When lines 10–11 and 13–14 are tripped, the wind turbine in bus 12 is insulated from the other parts of the distribution system, and thus, the total available wind power generation cannot be accommodated by total distribution system loads. In this case, if there are no P2G facilities in the joint scheduling distribution system, the distribution system will partially overcome this issue by wind power curtailment. Besides, if there are P2G facilities in the joint scheduling distribution system, the distribution system can overcome this issue by converting wind power generation into natural gas. Fig. 4 compares the wind power generation of the WT (i.e., the wind turbine in bus 12) without and with the P2G technology. The dashed curve indicates the total available WPG, the blue curve shows the WPG without P2G technology, and the orange curve illustrates the WPG with P2G technology integrated. Furthermore, the effect of the P2G technology on the electrical and gas operation cost values and electrical and gas load curtailment under the worst-case $N - k$ contingencies are compared in Tables 2 and 3. Tables 2 and 3 show the rapid decrease in the values of ELC, GLC, EOC, and GOC. Accordingly, the bidirectional energy flow caused by the P2G technology enhances the resilience of the combined gas and electrical networks considering the worst-case $N - k$ contingencies.

Table 3: Comparison of results for different $N-k$ contingencies; with P2G technology

$N-k$	EOC [k\$]	GOC [k\$]	ELC [MW]	GLC [kcf]	Computational burden [s]
3	1.03	0.97	8.12	21.23	110
4	1.72	1.11	19.23	34.67	144
5	1.98	1.43	76.32	88.55	170

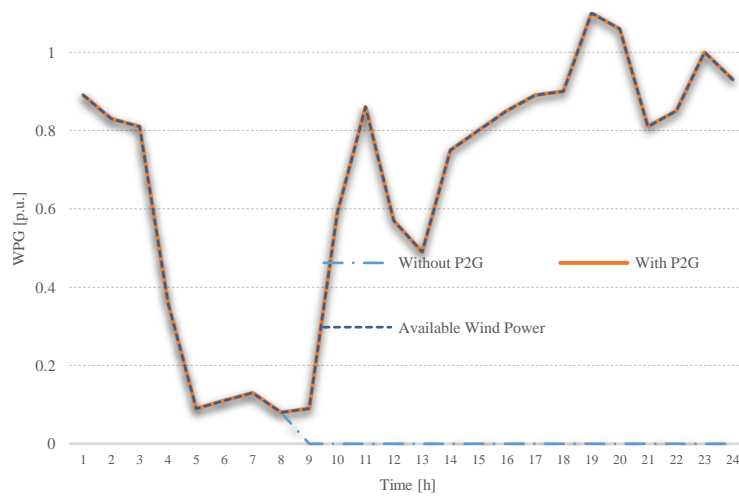


Fig. 4. Wind power accommodation without/with P2G technology.

C. Comparison of three operation methods for co-operation of the EDS&NGS

Three operation strategies for the min–max robust resilience-constrained co-operation of the EDS&NGS are compared in Tables 4 and 5. They compare the three operation strategies from the perspective of electrical and gas operation costs, load curtailments, the number of worst-case $N - k$ contingencies, and solution time. It should be noted that the decision-making in two energy systems is considered fully independent for the isolated method. Thus, the system operators operate autonomously without communication or sharing any data, whereas in the decentralized and centralized strategies the data can exchange among the EDS&NGS preserving information privacy. As shown in Table 3, there is a significant difference between the isolated strategy and the other two strategies under the worst-case $N - 3$ contingencies. Besides, small differences between the operation results of two decentralized and centralized strategies demonstrate the effectiveness of the proposed decentralized strategy.

The most interesting aspect of this table is the highest values for electrical and gas unserved loads detected for the isolated strategy, whereas the values are lowest for the centralized strategy. However, the reason for this result is that once we ignore data sharing between the two energy systems, the gas consumption of NGU-2 and the gas load at the same node, i.e., Node 7, are considerable during the operation process. Accordingly, there is a higher chance of a gas pressure loss and a natural gas shortage at Node 7 during periods 9 h–24 h because of the nonelectrical gas load and the electrical gas load, i.e., NGU-1, have simultaneously reached their peak values. To improve the gas pressures and supply gas loads at Node 7, there are two primary options: i) curtailment of the nonelectrical gas load at Node 7 and ii) reducing gas consumption of NGU-1 at the same node. As the gas load at Node 7 for the natural gas operator has the higher priority, consequently, just reducing the gas consumption of NGU-2 is the best option for the natural gas operators. In addition, a point often overlooked is that as mentioned above, extra wind power generation can be converted into gas with P2G technology and consumed with both NGUs and nonelectrical gas loads, but if data communication is ignored, this gas generation is only consumed with nonelectrical gas loads.

Table 4: Comparison of results for worst-case N-3 contingencies; with P2G technology.

Method	EOC [k\$]	GOC [k\$]	ELC [MW]	GLC [kcf]	Computational burden [s]
Decentralized	1.03	0.97	8.12	21.23	110
Centralized	1.01	0.97	8.09	21.23	78
Isolated	1.32	0.89	13.09	12.23	66

Table 5: Comparison of results for worst-case N-5 contingencies; with P2G technology.

Method	EOC [k\$]	GOC [k\$]	ELC [MW]	GLC [kcf]	Computational burden [s]
Decentralized	1.98	1.43	76.32	88.55	170
Centralized	1.97	1.42	75.12	86.16	130
Isolated	2.66	1.21	96.21	62.56	71

Under those circumstances, the energy generation of the NGUs in the EDS is reduced and the electrical load curtailment is increased. However, the shared data could enhance the gas pressure and reduce gas curtailment for NGU-1 at Node 7 by increasing gas injection to this node with P2G technology.

Tables 4 and 5 compare the isolated and centralized strategies under the worst-case $N - 3$ and $N - 5$ contingencies. The values of the operation costs and load curtailments for the isolated strategy under different worst-case $N - k$ contingencies are at the highest level for both operators. However, these values for decentralized and centralized strategies are at lower levels. Tables 4 and 5 show that the decentralized strategy has a more efficient capability to cover the worst-case $N - k$ contingencies in EDS operation, and it could provide a more resilient level for the EDS operator under the same worst-case $N - k$ contingencies. Similarly, the proposed decentralized strategy plays a more important role in preserving the decision-making independence and data privacy between both the energy system operators. Furthermore, data sharing between both the energy system operators is generally more time consuming in practice. When only restricted data are shared in the proposed decentralized strategy, communication burdens are mitigated for both decision-makers. Accordingly, a decentralized strategy is necessary for the co-operation of the EDS&NGS to demonstrate the effectiveness and necessity of this strategy.

B. 123-bus-20-node EDS&NGS

To illustrate the efficacy of the proposed method, the results of a relatively large-scale test energy systems are presented here to represent the computational and convergence performances of the proposed decentralized approach. Thus, a modified 123-bus-20-node EDS&NGS is presented to verify the effectiveness of the proposed models and decentralized approach. The modified 123-bus-20-node EDS&NGS has 124 transmission lines, 6 WT, 6 P2G, 5 NGUs, 2 gas wells, and 19 pipelines. More data for these energy systems can be found at motor.ece.iit.edu/data/123-bus-20-node.xlsx. The percent of hourly system load is the same as the pervious test EDS&NGS. Similar to previous test EDS&NGS, the new EDS&NGS based on the multi-zone and multi-time extreme hurricane model is divided into three zones, including three zones and three time periods. Noted that, the WTs and the P2G technologies are located at the same buses, i.e., [7, 52, 84, 97, 115,121]. The WT output profile and P2G capacity follow the same pattern as that of the previous energy systems. Similar to before test system, two set of the budgets of wind uncertainty $\alpha_t = 0.8, \forall t \in [8h, 16h]$, $\alpha_t = 0.2, \forall t \notin [8h, 16h]$ and worst-case $N - 3$ and $N - 9$ contingencies ($\eta_1 = \eta_2 = \eta_3 = 3$ and $\eta_1 = \eta_2 = \eta_3 = 3$) are considered to demonstrate the proposed multi-zone and multi-time extreme hurricane model for an larger test system. The decentralized, centralized, and isolated methods for 123-bus-20-node EDS&NGS in terms of the EOC, GOC, ELC, GLC and computation time are compared in Tables 6 and 7 for different $N-k$ contingencies.

The results of the centralized method, which are globally optimal, are served as the benchmark in Tables 8 and 9. It is apparent from this table that the solution results for the decentralized method need less computation time compared with the centralized method, although the scale of the new test system increases compared with the previous test energy systems, confirming its fast convergence features. What is interesting about the data in this table is that when the decentralized method is implemented

in a larger test system (i.e., 123-bus-20-node EDS&NGS), the computation advantages of the proposed decentralized method can be better unlocked which justifies the performance of the decentralized method against the system’s scale. Note that the computational time to solve the proposed min–max robust resilience-constrained co-optimization model relative to its accuracy is reasonable and vary good for the large-scale system. Also, to evaluate the convergence property and solution quality, the optimization results of the proposed decentralized approach for the previous and new test systems of EDS&NGS are shown in Fig. 5. Noted that, the EOC of the centralized method, which are globally optimal, are served as the benchmark in Tables 6 and 7. The most interesting aspect of this figure is that the maximum number of convergence iterations for the proposed decentralized approach in 33-bus-9-node energy systems is 10 and in the new modified 123-bus-20-node EDS&NGS is 16. Indeed, while the scale of EDS&NGS increases with a factor of 3.7, the number of iterations to converge and corresponding solution time for the proposed iterative proposed decentralized approach does not increase in a linear function of the scale of test system.

Table 6: Comparison of results for the worst-case N-3 contingencies; with P2G technology; modified 123-bus-20-node EDS&NGS.

Method	EOC [k\$]	GOC [k\$]	ELC [MW]	GLC [kcf]	Computational burden [s]
Decentralized	4.12	2.54	15.11	41.43	310
Centralized	4.11	2.55	15.12	41.43	806
Isolated	4.42	2.98	18.12	32.43	155

Table 7: Comparison of results for the worst-case N-9 contingencies; with P2G technology; modified 123-bus-20-node EDS&NGS.

Method	EOC [k\$]	GOC [k\$]	ELC [MW]	GLC [kcf]	Computational burden [s]
Decentralized	7.53	4.56	34.31	61.54	390
Centralized	7.51	4.54	34.32	61.53	1087
Isolated	7.82	4.98	26.21	53.34	183

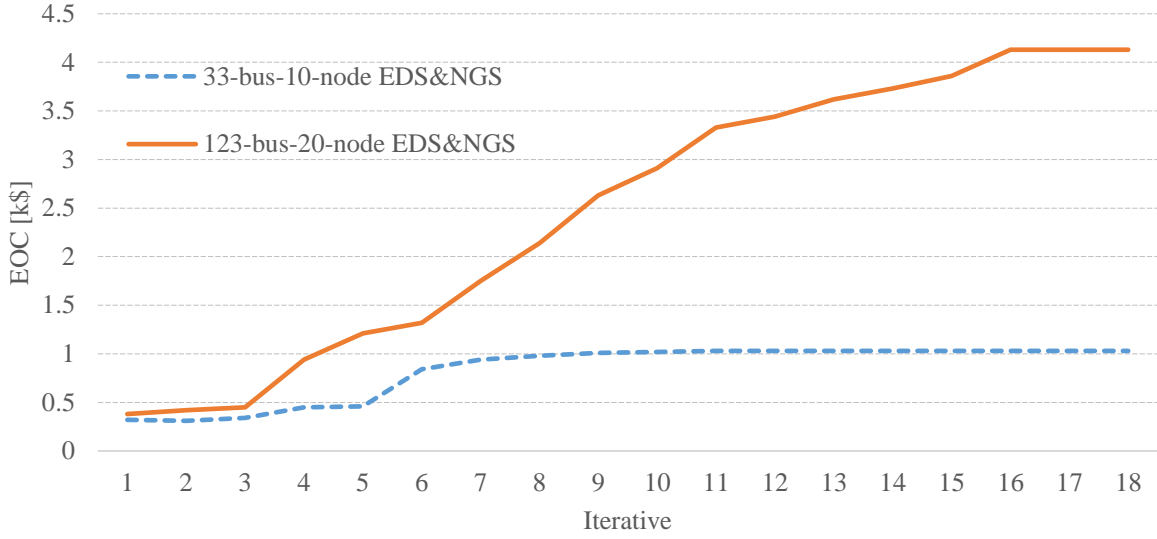


Fig. 5: Convergence of the proposed iterative decentralized approach.

VI. CONCLUSIONS

In this paper, a min–max robust co-optimization model was proposed to enhance the resilience of the co-operation of the EDS&NGS. The proposed model can identify the multi-zone and multi-time uncertainty set that includes worst-case $N - k$ contingencies and wind power generation uncertainty. The obtained results verify that utilization of the P2G technology can enhance the resilience of the co-operation of the EDS&NGS under worst-case $N - k$ contingencies by reducing electrical and gas load curtailment. Three operation strategies, i.e., isolated, centralized, and decentralized strategies were considered. The results demonstrate that the operation cost and load curtailment for both energy systems are at the highest level for the isolated strategy. However, the centralized strategy is at the lowest level among the three strategies. The obtained results for the centralized and decentralized strategies are almost the same with slight differences. The EDS&NGS can perform as independent entities with sharing a set of restricted information to preserve information privacy.

VII. APPENDIX

It should be noted that the model (47)-(54) is a bi-level optimization problem where the worst-case $N - k$ contingencies and extreme wind power uncertainty is found. Its abstract mathematical formulation can be given as follows:

$$\max_{U \in \{z, AP\}} \min_y b^T y \quad (78)$$

$$Hy \leq h \leftrightarrow \lambda \quad (79)$$

$$Az + By \leq g \leftrightarrow \varphi, \forall z \in \{0,1\} \quad (80)$$

$$Iy = d - \Delta p \leftrightarrow \gamma \quad (81)$$

$$Fz \leq n, \forall z \in \{0,1\} \quad (82)$$

$$\Delta p \leq p \quad (83)$$

where y indicates continuous variables and $\{z, \Delta p\}$ show discrete and continuous uncertain variables in the third level problem.

In fact, a continuous variable y is a vector of $\Xi_2 = \{P_{gt}^r, Q_{gt}^r, \vec{P}_t^r, \vec{Q}_t^r, \vec{P}_{ij,t}^r, \vec{Q}_{ij,t}^r, P_{ij,t}^r, Q_{ij,t}^r, V_{i,t}^r, \psi_{ij,t}^r, \phi_{ij,t}^r\}$ and the discrete and continuous uncertain variables $\{z, \Delta p\}$ are vectors of $\Xi_1 = \{P_{wt}^r, z_{kt}\}$ in Section 4. Constraint (79) includes dispatch related constraints such as constraints (13)-(19) and (27)-(28). Constraint (80) refers to line flow limit constraints such as constraints (20)-(26). Constraint (81) shows power balance at a bus which includes constraints (49)-(50). Constraints (82) and (83) represent the maximum limits for the discrete and continuous uncertain variables which includes constraints (1)-(6).

$$\max_{\{\varphi, \lambda, \gamma\}} -\lambda^T h - \varphi^T (g - Az) + \gamma^T (d - \Delta p) \quad (84)$$

$$-H \lambda^T - B \varphi^T + I \gamma^T = b^T \quad (85)$$

$$\varphi \geq 0, \lambda \geq 0, \gamma \text{ free} \quad (86)$$

$$(81)-(82) \quad (87)$$

The max-min problem (78)-(83) is transformed into a max-max problem. Also, it can be converted to a single equivalent dual problem based on the duality theory [42]. Also, the continuous variables φ, λ, γ are the dual variables of the constraints (79)–(83), respectively.

ACKNOWLEDGEMENT

The authors thank Dr. Hanna Niemelä for her assistance with proof-reading of the paper and comments that greatly improved the manuscript.

REFERENCES

- [1] H. Raoufi, V. Vahidinasab, and K. Mehran, "Power systems resilience metrics: A comprehensive review of challenges and outlook," *Sustainability*, vol. 12, no. 22, p. 9698, 2020.
- [2] Economic Benefits of Increasing Electric Grid Resilience to Weather Outages, August, <http://energy.gov/downloads/economic-benefitsincreasing-electric-grid-resilience-weather-outages>, 2013.
- [3] A. Nikoobakht, J. Aghaei, M. Shafie-khah, and J. Catalão, "Continuous-Time Co-Operation of Integrated Electricity and Natural Gas Systems with Responsive Demands Under Wind Power Generation Uncertainty," *IEEE Transactions on Smart Grid*, 2020.
- [4] A. Nikoobakht and J. Aghaei, "IGDT-based robust optimal utilisation of wind power generation using coordinated flexibility resources," *IET Renewable Power Generation*, vol. 11, no. 2, pp. 264-277, 2016.
- [5] G. Li, R. Zhang, T. Jiang, H. Chen, L. Bai, and X. Li, "Security-constrained bi-level economic dispatch model for integrated natural gas and electricity systems considering wind power and power-to-gas process," *Applied energy*, vol. 194, pp. 696-704, 2017.
- [6] R.-P. Liu, S. Lei, C. Peng, W. Sun, and Y. Hou, "Data-Based Resilience Enhancement Strategies for Electric-Gas Systems Against Sequential Extreme Weather Events," *IEEE Transactions on Smart Grid*, vol. 11, no. 6, pp. 5383-5395, 2020.
- [7] A. R. Sayed, C. Wang, and T. Bi, "Resilient operational strategies for power systems considering the interactions with natural gas systems," *Applied Energy*, vol. 241, pp. 548-566, 2019.
- [8] C. Shao, M. Shahidepour, X. Wang, X. Wang, and B. Wang, "Integrated planning of electricity and natural gas transportation systems for enhancing the power grid resilience," *IEEE Transactions on Power Systems*, vol. 32, no. 6, pp. 4418-4429, 2017.
- [9] B. Zou, C. Wang, Y. Zhou, J. Wang, C. Chen, and F. Wen, "Resilient co-expansion planning between gas and electric distribution networks against natural disasters," *IET Generation, Transmission & Distribution*, vol. 14, no. 17, pp. 3561-3570, 2020.
- [10] W. Yuan, J. Wang, F. Qiu, C. Chen, C. Kang, and B. Zeng, "Robust optimization-based resilient distribution network planning against natural disasters," *IEEE Transactions on Smart Grid*, vol. 7, no. 6, pp. 2817-2826, 2016.
- [11] A. Nasri, A. Abdollahi, and M. Rashidinejad, "Multi-stage and resilience-based distribution network expansion planning against hurricanes based on vulnerability and resiliency metrics," *International Journal of Electrical Power & Energy Systems*, vol. 136, p. 107640, 2022.

- [12] X. Wang, Z. Li, M. Shahidehpour, and C. Jiang, "Robust line hardening strategies for improving the resilience of distribution systems with variable renewable resources," *IEEE Transactions on Sustainable Energy*, vol. 10, no. 1, pp. 386-395, 2017.
- [13] Y. Wang, L. Huang, M. Shahidehpour, L. L. Lai, H. Yuan, and F. Y. Xu, "Resilience-constrained hourly unit commitment in electricity grids," *IEEE Transactions on Power Systems*, vol. 33, no. 5, pp. 5604-5614, 2018.
- [14] M. Aien, A. Hajebrahimi, and M. Fotuhi-Firuzabad, "A comprehensive review on uncertainty modeling techniques in power system studies," *Renewable and Sustainable Energy Reviews*, vol. 57, pp. 1077-1089, 2016.
- [15] C. Wang *et al.*, "Robust defense strategy for gas–electric systems against malicious attacks," *IEEE Transactions on Power Systems*, vol. 32, no. 4, pp. 2953-2965, 2016.
- [16] W. van Ackooij, I. Danti Lopez, A. Frangioni, F. Lacalandra, and M. Tahanan, "Large-scale unit commitment under uncertainty: an updated literature survey," *Annals of Operations Research*, vol. 271, no. 1, pp. 11-85, 2018.
- [17] M. Tahanan, W. van Ackooij, A. Frangioni, and F. Lacalandra, "Large-scale unit commitment under uncertainty: a literature survey," 2014.
- [18] M. E. Parast, M. H. Nazari, and S. H. Hosseinian, "Resilience Improvement of Distribution Networks Using a Two-Stage Stochastic Multi-Objective Programming via Microgrids Optimal Performance," *IEEE Access*, vol. 9, pp. 102930-102952, 2021.
- [19] Q. Zhang, Z. Wang, S. Ma, and A. Arif, "Stochastic pre-event preparation for enhancing resilience of distribution systems," *Renewable and Sustainable Energy Reviews*, vol. 152, p. 111636, 2021.
- [20] M. Movahednia, A. Kargarian, C. E. Ozdemir, and S. C. Hagen, "Power Grid Resilience Enhancement via Protecting Electrical Substations Against Flood Hazards: A Stochastic Framework," *IEEE Transactions on Industrial Informatics*, vol. 18, no. 3, pp. 2132-2143, 2021.
- [21] Y. He, M. Shahidehpour, Z. Li, C. Guo, and B. Zhu, "Robust constrained operation of integrated electricity-natural gas system considering distributed natural gas storage," *IEEE Transactions on Sustainable Energy*, vol. 9, no. 3, pp. 1061-1071, 2017.
- [22] S. D. Manshadi and M. E. Khodayar, "Resilient operation of multiple energy carrier microgrids," *IEEE Transactions on Smart Grid*, vol. 6, no. 5, pp. 2283-2292, 2015.
- [23] A. Street, F. Oliveira, and J. M. Arroyo, "Contingency-constrained unit commitment with $n-k$ security criterion: A robust optimization approach," *IEEE Transactions on Power Systems*, vol. 26, no. 3, pp. 1581-1590, 2010.
- [24] A. Moreira, A. Street, and J. M. Arroyo, "An adjustable robust optimization approach for contingency-constrained transmission expansion planning," *IEEE Transactions on Power Systems*, vol. 30, no. 4, pp. 2013-2022, 2014.
- [25] X. Wu, A. J. Conejo, and N. Amjady, "Robust security constrained ACOPF via conic programming: Identifying the worst contingencies," *IEEE Transactions on Power Systems*, vol. 33, no. 6, pp. 5884-5891, 2018.
- [26] F. Qi, M. Shahidehpour, Z. Li, F. Wen, and C. Shao, "A chance-constrained decentralized operation of multi-area integrated electricity–natural gas systems with variable wind and solar energy," *IEEE Transactions on Sustainable Energy*, vol. 11, no. 4, pp. 2230-2240, 2019.
- [27] V. Shabazbegian, H. Ameli, M. T. Ameli, G. Strbac, and M. Qadrdan, "Co-optimization of resilient gas and electricity networks; a novel possibilistic chance-constrained programming approach," *Applied Energy*, vol. 284, p. 116284, 2021.
- [28] C. He, C. Dai, L. Wu, and T. Liu, "Robust network hardening strategy for enhancing resilience of integrated electricity and natural gas distribution systems against natural disasters," *IEEE Transactions on Power Systems*, vol. 33, no. 5, pp. 5787-5798, 2018.
- [29] E. A. Javadi, M. Joorabian, and H. Barati, "A bi-level optimization framework for resilience enhancement of electricity and natural gas networks with participation of energy hubs," *International Journal of Electrical Power & Energy Systems*, vol. 142, p. 108312, 2022.
- [30] M. Ansari, M. Zadsar, H. Zareipour, and M. Kazemi, "Resilient operation planning of integrated electrical and natural gas systems in the presence of natural gas storages," *International Journal of Electrical Power & Energy Systems*, vol. 130, p. 106936, 2021.
- [31] National Hurricane Center. (Apr. 29, 2015). Hurricane Decay: Demise of a Hurricane. [Online]. Available: <http://www.hurricanescience.org/science/science/hurricanedecay/>.
- [32] A. Nikoobakht, J. Aghaei, and M. Mardaneh, "Securing highly penetrated wind energy systems using linearized transmission switching mechanism," *Applied Energy*, vol. 190, pp. 1207-1220, 2017.
- [33] D. Bertsimas, E. Litvinov, X. A. Sun, J. Zhao, and T. Zheng, "Adaptive robust optimization for the security constrained unit commitment problem," *IEEE transactions on power systems*, vol. 28, no. 1, pp. 52-63, 2012.
- [34] S. Tosserams, L. Etman, P. Papalambros, and J. Rooda, "An augmented Lagrangian relaxation for analytical target cascading using the alternating direction method of multipliers," *Structural and multidisciplinary optimization*, vol. 31, no. 3, pp. 176-189, 2006.
- [35] M. Razaviyayn, T. Huang, S. Lu, M. Nouiehed, M. Sanjabi, and M. Hong, "Nonconvex min-max optimization: Applications, challenges, and recent theoretical advances," *IEEE Signal Processing Magazine*, vol. 37, no. 5, pp. 55-66, 2020.
- [36] A. Nikoobakht, J. Aghaei, M. Parvania, and M. Sahraei-Ardakani, "Contribution of FACTS devices in power systems security using MILP-based OPF," *IET Generation, Transmission & Distribution*, vol. 12, no. 15, pp. 3744-3755, 2018.

- [37] X. Luo, S. Xia, K. W. Chan, and X. Lu, "A hierarchical scheme for utilizing plug-in electric vehicle power to hedge against wind-induced unit ramp cycling operations," *IEEE Transactions on Power Systems*, vol. 33, no. 1, pp. 55-69, 2017.
- [38] Y. He *et al.*, "Decentralized optimization of multi-area electricity-natural gas flows based on cone reformulation," *IEEE Transactions on Power Systems*, vol. 33, no. 4, pp. 4531-4542, 2017.
- [39] N. Michelena, H. Park, and P. Y. Papalambros, "Convergence properties of analytical target cascading," *AIAA journal*, vol. 41, no. 5, pp. 897-905, 2003.
- [40] D. P. Bertsekas, "Nonlinear programming," *Journal of the Operational Research Society*, vol. 48, no. 3, pp. 334-334, 1997.
- [41] GAMS. The Solver Manuals. 1996 [Online]. Available: <http://www.gams.com/>.
- [42] D. Bertsimas, E. Litvinov, X. A. Sun, J. Zhao, and T. Zheng, "Adaptive robust optimization for the security constrained unit commitment problem," *IEEE Transactions on Power Systems*, vol. 28, no. 1, pp. 52-63, 2013.